Effects of linear amphiphilicity on membrane interactions of C-terminal thrombin peptides

Singh, Shalini; Papareddy, Praveen; Kalle, Martina; Schmidtchen, Artur; Malmsten, Martin

Published in:
RSC Advances

DOI:
10.1039/c4ra05420b

2014

Effects of linear amphiphilicity on membrane interactions of C-terminal thrombin peptides

Shalini Singh[1,*], Praveen Papareddy[2], Martina Kalle[2], Artur Schmidtchen[2,3], and Martin Malmsten[1]

[1]Department of Pharmacy, Uppsala University, SE-75123, Uppsala, Sweden

[2]Division of Dermatology and Venereology, Department of Clinical Sciences, Lund University, SE-221 84 Lund, Sweden, [3]Dermatology, LKCMedicine, Nanyang Technological University, Singapore 308232

.

[*]Corresponding author. Tel: +46184714368; Fax: +46184717725; E-mail: shalini.singh@farmaci.uu.se

Key words: amphiphilicity, antimicrobial peptide, dual polarization interferometry, ellipsometry, membrane

Abstract

Effects of linear amphiphilicity on membrane interactions of antimicrobial peptides were investigated by ellipsometry, dual polarization interferometry, fluorescence spectroscopy, light scattering, and circular dichroism. In doing so, the thrombin-derived GKY25 (GKYGFYTHVFRLKKWIQKVIDQFGE) was compared to WFF25 (WFFFYYLIIGGGVVTHQQRKKKKDE) of identical composition, but with amino acids sorted according to hydrophobicity, the latter peptide thus displaying pronounced linear amphiphilicity. In addition, GKY25d (GKYG(f)YTH(v)FRL(k)KWI(q)KVI(d)QFGE; with identical sequence but with selected D-amino acid substitutions) was included as a control peptide, for which conformationally induced (helix-related) amphiphilicity was suppressed. Through its pronounced linear amphiphilicity, WFF25, but not the less amphiphilic GKY25 and GKY25d, forms aggregates in solution. Through its terminal W/F stretch, WFF25 also displays pronounced selectivity, with higher membrane binding and liposome rupture than GKY25 and GKY25d for anionic membranes, but suppressed peptide insertion and lytic effects for zwitterionic ones. In addition, WFF25 binds extensively to anionic polyelectrolyte components in bacterial membranes, i.e., lipopolysaccharide and lipoteichoic acid, resulting in reduced antimicrobial effects through peptide scavenging, not seen for the less amphiphilic GKY25 and GKY25d peptides. Taken together, the results thus demonstrate a series of striking effects for highly amphiphilic peptides, which need to be recognized in the development of such compounds as potential peptide therapeutics.

Introduction

The increasing occurrence of multidrug resistant bacteria (1,2) has become a growing concern, prompting an urgent need for novel antimicrobials. Antimicrobial peptides (AMPs) constitute one such class of potential anti-infective drugs, and are currently receiving much attention in both academic research and drug development (3-8). AMPs have been identified from a number of sources, including plants (9), insects (10), and vertebrates (11). Currently, significant interest is directed towards AMPs of endogenous origin, such as defensins, cathelicidins, and histatins (12,13). In the latter context, AMP sequences found in endogenous proteins, including complement, coagulation, and matrix proteins, have attracted interest, since several of these have been found to display potent antimicrobial effects, yet not provoking extensive toxicity (14-18). Findings from these and other studies have suggested that such molecules may indeed be generated by infection-triggered proteolytic degradation of endogenous proteins by bacterial or host defense cell-related enzymes.

Motivated by the need of AMPs with potent and selective antimicrobial effects, but also added biological functionalities, we previously identified GKY25 (GKYGFYTHVFRLKKWIQKVIDQFGE), derived from the C-terminus of human thrombin, as a peptide displaying interesting antimicrobial and anti-inflammatory effects (16). In an attempt to elucidate the origin of anti-inflammatory properties of this peptide, its interaction with bacterial lipopolysaccharide (LPS) and its lipid A moiety was subsequently investigated (19). While the extent of LPS or lipid A binding was demonstrated not to be sole discriminant for the anti-endotoxic effect of these peptides, helix formation in peptide/LPS complexes, as well as peptide-induced LPS micelle disintegration, were demonstrated to correlate to the anti-endotoxic effect of these peptides.

In the present investigation, attention is shifted to membrane interactions and antimicrobial effects of GKY25 and its variants, notably the effects of linear amphiphilicity. There is by now a considerable literature on how peptide physicochemical properties such as length, charge, hydrophobicity, and secondary structure affect peptide-membrane interaction and resulting antimicrobial activity, as well as an increasing number of corresponding studies on acyl-modified lipopeptides, for which self-assembly expectedly influence membrane interactions (3). In contrast, there are essentially no studies in literature addressing membrane interactions of peptides displaying a hydrophobicity gradient along its chain, i.e., for which the linear amphiphilicity is introduced within the peptide sequence. For peptides displaying a gradual progression from hydrophobic to hydrophilic along the peptide chain, both self-assembly and its consequences for membrane interactions become complex issues, which have yet to be elucidated. This was therefore the main aim of the present study.

In order to clarify the effects of linear amphiphilicity on membrane interactions, GKY25 (GKYGFYTHVFRLKKWIQKVIDQFGE) was compared to WFF25 (WFFFYYLIIGGGVVTHQQRKKKKDE) of identical composition, but with amino acids sorted according to hydrophobicity, the latter peptide thus displaying pronounced linear amphiphilicity. In addition, GKY25d (GKYG(f)YTH(v)FRL(k)KWI(q)KVI(d)QFGE; with identical sequence but with selected D-amino acid substitutions (denoted lower case)) was included as a control peptide, for which conformationally induced (helix-related) amphiphilicity was suppressed. Membrane interactions were investigated using a method combination of ellipsometry, dual polarization interferometry (DPI), circular dichroism spectroscopy (CD), fluorescence spectroscopy, dynamic light scattering, and nanoparticle tracking

analysis, and results were compared to those on antimicrobial effects. In particular, the investigation offers some physicochemical insight into how extreme peptide linear amphiphilicity affects membrane interactions and antimicrobial effects.

Experimental

Chemicals. Peptides (GKYGFYTHVFRLKKWIQKVIDQFGE) (GKY25), (GKYG(f)YTH(v)FRL(k)KWI(q)KVI(d)QFGE) (GKY25d; D substitutions denoted lower case), and WFFFYYLIIGGGVVTHQQRKKKKDE (WFF25) (Table 1), were all synthesized by Biopeptide Co. (San Diego, USA), and were of >95% purity, as evidenced by mass spectral analysis (MALDI-TOF Voyager). LPS from *Escherichia coli* (0111:B4) and lipoteichoic acid (LTA) from *Staphylococcus aureus* were both from Sigma (St. Louis, USA).

Microorganisms. *E. coli* (ATCC 25922), *Pseudomonas aeruginosa* (ATCC 27853), and *S. aureus* (ATCC 29213) were obtained from the Department of Clinical Bacteriology at Lund University Hospital, Sweden.

Viable count analysis (VCA). Bacteria (*E. coli*, *P. aeruginosa,* and *S. aureus*) were grown to mid-logarithmic phase in Todd-Hewitt (TH). Subsequently, they were washed and diluted in 10 mM Tris, pH 7.4, either alone or with 10 mM Tris, pH 7.4, containing 0.15 M NaCl. 2 x 10^6 cfu/mL bacteria were incubated in 50 μL at 37°C for 2 h with peptides at the indicated concentrations. Serial dilutions of the incubation mixture were plated on TH agar, followed by incubation at 37°C overnight and cfu determination.

Liposome preparation and leakage assay. The liposomes investigated were either anionic (DOPE/DOPG 75/25 mol/mol or *E. coli* polar lipid extract), or zwitterionic (DOPC or DOPC/cholesterol 60/40 mol/mol). DOPG (1,2-dioleoyl-*sn*-Glycero-3-phosphoglycerol, monosodium salt), DOPE (1,2-dioleoyl-*sn*-Glycero-3-phosphoetanolamine), DOPC (1,2-dioleoyl-*sn*-Glycero-3-phosphocholine), and *E. coli* polar lipid extract (67% phosphatidylethanolamine, 23.2% phosphatidylglycerol and 9.8% cardiolipin) were from Avanti Polar Lipids (Alabaster, USA) and of >99% purity, while cholesterol (>99% purity) was from Sigma-Aldrich (St. Louis, USA). 5(6)-carboxyfluorescein (CF) was from Sigma-Aldrich (St. Louis, USA) and of >95% purity. The lipid mixtures were dissolved in chloroform, after which solvent was removed by evaporation under vacuum overnight. Subsequently, 10 mM Tris buffer, pH 7.4 (with or without additional 150 mM NaCl), was added together with 0.1 M carboxyfluorescein (CF). After hydration, the lipid mixture was subjected to eight freeze-thaw cycles (not for *E. coli* liposomes, since these were unable to withstand this process), consisting of freezing in liquid nitrogen followed by heating to 60°C. Unilamellar liposomes were generated by multiple extrusions (30 passages) through polycarbonate filters (pore size 100 nm) mounted in a LipoFast miniextruder (Avestin, Ottawa, Canada) at 22°C. Untrapped CF was removed by two subsequent gel filtrations (Sephadex G-50, GE Healthcare, Uppsala, Sweden) at 22°C, with Tris buffer as eluent. CF release from the liposomes was determined by monitoring the emitted fluorescence at 520 nm from a liposome dispersion (10 μM lipid in 10 mM Tris, pH 7.4). Liposomes thus prepared displayed excellent stability, with a background release of 1-3%, (≈5-10% for *E. coli* liposomes). An absolute leakage scale was obtained by disrupting the liposomes at the end of each experiment through addition of 0.8 mM Triton X-100 (Sigma-Aldrich, St. Louis, USA). A SPEX-

fluorolog 1650 0.22-m double spectrometer (SPEX Industries, Edison, USA) was used for the liposome leakage assay. Measurements were performed in triplicate at 37 °C.

CD spectroscopy. Circular dichroism (CD) spectra were measured by a Jasco J-810 Spectropolarimeter (Jasco, Easton, USA). Measurements were performed in a 10 mm quartz cuvette under stirring with a peptide concentration of 10 μM, both in 10 mM Tris and in presence of liposomes. The effect on peptide secondary structure of liposomes at a lipid concentration of 100 μM was monitored in the range 200-260 nm (wavelengths lower than this precluded due to light scattering by the ≈100 nm liposomes). Secondary structure content was analysed by K2D3 (20), which is based on comparing the CD spectrum of a peptide/protein to a reference set consisting of CD spectra of peptides/proteins of known structure. Theoretical CD spectra of a non-redundant set of structures representing most proteins in the Protein Data Bank is used as reference set in K2D3, resulting in improved predictions, particularly for beta-strand content. To account for instrumental differences between measurements, as well as signals from the bulk solution, background subtractions were performed routinely. All measurements were performed in duplicate at 37 °C.

Ellipsometry. Peptide adsorption to supported lipid bilayers was studied *in situ* by null ellipsometry (21), using an Optrel Multiskop (Optrel, Kleinmachnow, Germany) equipped with a 100 mW Nd:YAG laser (Uniphase). All measurements were carried out at 532 nm and an angle of incidence of 67.66° in a 5 mL cuvette under stirring (300 rpm). Both the principles of null ellipsometry and the procedures used have been described before (22). In brief, by monitoring the change in the state of polarization of

light reflected at a surface in the absence and presence of an adsorbed layer, the mean refractive index (n) and layer thickness (d) of the adsorbed layer can be obtained. From the thickness and refractive index, the adsorbed amount (Γ) was calculated according to:

$$\Gamma = \frac{(n - n_0)}{dn/dc} d \qquad (1)$$

where dn/dc is the refractive index increment (0.154 cm^3/g) and n_0 is the refractive index of the bulk solution. Corrections were routinely done for changes in bulk refractive index caused by changes in temperature and excess electrolyte concentration.

Supported lipid bilayers were generated from liposome adsorption. DOPE/DOPG (75/25 mol/mol) were prepared as described above, but the dried lipid films re-suspended in Tris buffer only with no CF present. In order to avoid adsorption of peptide directly at the silica substrate (surface potential -40 mV, and contact angle <10°) (23) through any defects of the supported lipid layer, poly-L-lysine (M_w = 170 kDa, Sigma-Aldrich, St. Louis, USA) was preadsorbed from water prior to lipid addition to an amount of 0.045 ± 0.01 mg/m^2, followed by removal of non-adsorbed poly-L-lysine by rinsing with water at 5 mL/min for 20 min (24). Water in the cuvette was then replaced by 10 mM Tris, pH 7.4, containing also 150 mM NaCl, which was followed by liposome addition at a lipid concentration of 20 μM. The final layer formed after 2 h had structural characteristics (thickness 4±1 nm, mean refractive index 1.47±0.03), suggesting that a layer fairly close to a complete bilayer is formed. After lipid bilayer formation, the cuvette was rinsed by 10 mM Tris buffer containing 150 mM NaCl at a rate of 5 mL/min over a period of 30 min. After stabilization for 40

min, peptide was added to a concentration of 0.01 μM, followed by three subsequent peptide additions to 0.1 μM, 0.5 μM, and 1 μM, in all cases monitoring the adsorption for one h. All measurements were made in at least duplicate at 25°C.

LPS-coated surfaces were prepared by adsorbing *E. coli* LPS to methylated silica surfaces (surface potential -40 mV, contact angle 90°) (23) from 0.4 mg/mL in 10 mM Tris, 150 mM NaCl, pH 7.4, over a period of 2 h. This results in a hydrophobically driven LPS adsorption of 1.48±0.38 mg/m^2, corresponding to plateau in the LPS adsorption isotherm under these conditions, with an approximate area per acyl group of 200 Å^2, assuming an LPS molecular weight of 10^4, and 6 acyl chains per LPS. Non-adsorbed LPS was removed by rinsing with Tris buffer at 5 mL/min for a period of 30 min, allowing buffer stabilization for 20 min. Peptide addition was performed at different concentrations of 0.01, 0.1, 0.5, and 1 μM, and the adsorption monitored for one h after each addition. All measurements were performed in at least duplicate at 25°C.

LTA-coated surfaces were obtained by preadsorption of poly-L-lysine to silica and subsequent rinsing, as described above, followed by adsorption of *S. aureus* LTA at 200 ppm in 10 mM Tris, 150 mM NaCl, pH 7.4. This results in an LTA adsorption of 1.05± 0.11 mg/m^2, corresponding to saturation in the LTA adsorption isotherm. Non-adsorbed LTA was removed by rinsing with buffer at 5 mL/min for a period of 20 min, followed by stabilization for 20 min. Peptide addition was subsequently performed to 0.01, 0.1, 0.5, and 1μM, and adsorption monitored for at least one h after each addition. All measurements were performed in at least duplicate at 25°C.

Dual polarization interferometry. Peptide incorporation into DOPE/DOPG, DOPC, and DOPC/cholesterol supported bilayers was investigated by dual polarization interferometry (DPI), using a Farfield AnaLight 4D (Biolin Farfield, Manchester, U.K.), operating with an alternating 632.8 nm laser beam. The technique is based on a dual slab waveguide, consisting of an upper sensing waveguide (supporting the lipid bilayer) and a lower reference waveguide. The changes induced by the peptide/lipid adsorption was monitored through changes in the transverse electric and transverse magnetic modes, as described previously (25). As for ellipsometry, Eq. 1 was used for determining the mass adsorbed, using a refractive index increment of 0.154 cm^3/g. Although treating phospholipids as optically isotropic systems is a reasonably accurate approximation for disorganized phospholipid bilayers, these actually display some optical birefringence, which is measurable with the sensitive DPI technique. The birefringence (Δn_f), obtained from the refractive indices for the TM and TE waveguide modes (assuming the bilayer thickness to be constant), reflects ordering of the lipid molecules in the bilayer, and decreases with increasing disordering of the bilayer (26,27). Consequently, Δn_f can be used to monitor ordering transitions in lipid bilayers as a result of peptide binding and incorporation, and therefore offers a simpler alternative to, e.g., order parameter analyses in ^{2}H-NMR spectroscopy (28). In the present study, DOPE/DOPG (75/25 mol/mol), DOPC, and DOPC/cholesterol (60/40 mol/mol) liposomes were prepared as described above for ellipsometry, and the liposomes (at a lipid concentration of 0.2 mg/mL in 10 mM HEPES buffer, pH 7.4, containing 150 mM NaCl and 1.5 mM $CaCl_2$) fused to the silicon oxynitride/silicon substrate (contact angle $<5^0$) at a flow rate of 25 μL/min for 8 min. This resulted in bilayer formation, characterized by a refractive index of 1.47, a thickness of 4.5±0.3 nm, and an adsorbed amount of 4.4±0.3 $\mu g/m^2$ (corresponding to

an area per molecule of 54 $Å^2$). After bilayer formation, the buffer was replaced by 10 mM Tris buffer, pH 7.4, during continuous flushing at 50 μL/min for 10 min, after which peptide was added at the desired concentration. All measurements were made in at least duplicate at 25°C.

Size measurements. The mean diameter of peptide aggregates was determined by dynamic light scattering at a scattering angle of 173°, using a Zetasizer Nano ZS (Malvern Instruments, Malvern, UK). Measurements were performed in duplicate at 25°C and a fixed peptide concentration of 10 μM in 10 mM Tris, pH 7.4. In addition, size determination of DOPE/DOPG, DOPC, and DOPC/cholesterol liposomes at different peptide concentrations was performed by nanoparticle tracking analysis (NTA), using a NanoSight NS500 (NanoSight Ltd., Amesbury, UK), equipped with a 75 mW laser at 532 nm, and the NTA 2.3 analytical software. Within an illumination device mounted under a microscope, particles passing through the beam path are visualized as small dots. From the displacements measured, diffusion coefficients of individual particles are obtained, the size of which is subsequently obtained from the Stokes-Einstein equation. The lipid concentration used for sample preparation was 10 μM, and measurements performed at 22°C, 1h after sample preparation. Due to low particle concentration necessary for NTA (10^8-10^9 particles/mL), samples were diluted with 10 mM Tris, pH 7.4, just prior to measurement. Each size measurement was based on a 30 s video, analyzed using a screen gain of 10, blur: auto, and a detection threshold of 8-10. Data are presented as the average and standard deviation of the three video recordings.

Fluorescence spectra. Tryptophan fluorescence spectra were determined by a Spex fluorolog 1680 0.22m double spectrometer (Instruments S. A. Group, Edison, USA). The excitation wavelength used was 280 nm, and emission spectra recorded between 300 and 450 nm. Measurements were performed at a 10 μM peptide concentration at 37°C under continuous stirring in 10 mM Tris, pH 7.4, with and without 150 mM NaCl. Subsequently, liposomes (100 μM lipid, giving the same peptide-to-lipid ratio as during leakage experiments at a peptide concentration of 1 μM), were included and the spectra recorded.

Results

Adsorption. Shown in Fig. 1 are results on the adsorption of GKY25, GKY25d, and WFF25 at model anionic DOPE/DOPG bilayers at physiological ionic strength. As shown, the adsorption of GKY25 and GKY25d is quite similar at these highly negatively charged bilayers (z≈-40 mV) (29). WFF25, on the other hand, displays a much higher adsorption density at these highly screened conditions due to its linear amphiphilicity and hydrophobic tail. Further addressing the issue of the effects of lipid head group composition on peptide binding, DPI experiments were performed, wherein phospholipid head group charge and membrane sterol content were varied (Fig. 2). For all membrane compositions investigated, peptide addition results in a monotonous decrease in bilayer birefringence with increasing peptide adsorption, without any threshold adsorption required for peptide insertion into the lipid membrane. Also independent of membrane composition, GKY25 and GKY25d induce similar membrane disorganization at a given adsorption density, while WFF25 induces less membrane disordering. According to Fig. 2, maximum adsorption of WFF25 at anionic DOPE/DOPG membranes (≈ 600 nmol at the point of experiment

termination) is larger than that of GKY25 and GKY25d (≈ 350 nmol), as also seen with ellipsometry at higher ionic strength. For zwitterionic DOPC/cholesterol membranes, in contrast, the W/F-rich terminus of WFF25 suppresses adsorption compared to GKY25 and GKY25d, as discussed further below.

Liposome leakage. To further investigate the correlation between peptide adsorption and membrane rupture, liposome leakage experiments were performed. As shown in Figs. 3 and S1, all three peptides induce concentration-dependent liposome permeabilization. For anionic DOPE/DOPG and *E. coli* liposomes, a notably higher leakage induction is observed for the more amphiphilic WFF25, particularly clearly seen at high ionic strength. These results mirror those obtained on peptide binding by ellipsometry and DPI. At high peptide concentrations, colloidal destabilization of these liposomes is observed in the case of WFF25, but not for GKY25 and GKY25d (Fig. S2). Due to a lower adsorption density, peptide-induced flocculation was not seen for the zwitterionic liposomes. Comparing liposome leakage for GKY25 and GKY25d, we note that GKY25 displays more pronounced membrane rupturing than GKY25d for the zwitterionic DOPC and DOPC/cholesterol liposomes, illustrating that the partial formation of a (modestly) amphiphilic helix by GKY25 but not GKY25d (Table 2, Figures S3 and S4) contributes to peptide binding and membrane disruption, but only for systems where electrostatics has been largely suppressed. Interestingly, this difference between GKY25 and GKY25d is observed also for the relatively less stable *E. coli* liposomes, but not for the more robust DOPE/DOPG ones.

Antimicrobial Effects. To investigate the correlation between membrane rupture and antimicrobial effect, viable count experiments were performed. As shown in Figs. 4 and S5, GKY25 displays potent antimicrobial effects for Gram-negative *E. coli* and *P. aeruginosa,* as well as Gram-positive *S. aureus*, although decreasing with increasing ionic strength. Quantitatively, the antimicrobial effects for GKY25, GKY25d, and WFF25 are comparable at low ionic strength, whereas WFF25 and GKY25d are much more sensitive to increasing ionic strength than GKY25 for all strains investigated. Comparing *E. coli* liposome leakage and bacterial killing, GKY25 is more potent in both cases than GKY25d, illustrating the importance of helix formation for membrane destabilization for these peptides at high ionic strength. In contrast, WFF25, the most potent of peptides in terms of lysis of anionic ("bacteria mimicking") liposomes, induces the *weakest* bacterial killing at high ionic strength. Considering the high adsorption density of the highly amphiphilic WFF25 at anionic lipid membranes (Figs. 1 and 2), adsorption-induced liposome flocculation may at first be thought to result in an additional driving force for membrane disruption of liposomes, not present for bacteria. However, flocculation is not observed at 1 μM (Fig. S2), at which full leakage induction occurs for WFF25 for the anionic liposomes (Fig. 3A), but only at much higher peptide concentrations. Thus, peptide-induced liposome flocculation/fusion does not contribute to the leakage observed.

Instead, the observed difference between liposome and bacteria lysis is due to non-lipid components in the bacterial membrane. Thus, bacteria contain considerable amounts of membrane components not present in the model liposomes, notably LPS in Gram-negative bacteria and LTA in Gram-positive bacteria (30,31). These are highly anionic polyelectrolytes containing also hydrophobic domains, and display

very high binding capacity of WFF25, but considerably smaller for the less amphiphilic GKY25 and GKY25d (Fig. 5). In contrast to bacteria membranes, the model liposomes do not contain any LPS and LTA, hence no such scavenging occurs, and rupture is determined by peptide binding to the lipid bilayer only. This precludes comparison between liposome leakage experiments and antimicrobial results, but only for the highly amphiphilic WFF25.

WFF25 self-assembly. With its high linear amphiphilicity, WFF25 is somewhat similar to peptide amphiphiles, and is also able to self-assemble into aggregates. Thus, as shown in Fig. 6, light scattering experiments show that WFF25 is present as ≈30 nm aggregates at low ionic strength, whereas the less amphiphilic GKY25 and GKY25d are both present as individual molecules. An increase in WFF25 aggregate size was furthermore observed with increasing ionic strength. These results were further supported by W fluorescence results. Thus, for GKY25 and GKY25d, the wavelength at maximum W fluorescence intensity in aqueous solution (λ_{max}=352 nm and 351 nm, respectively) indicates maximum exposure of the W residues to the aqueous solvent for these peptides (32). In contrast, WFF25 displays a shift of λ_{max} to 345 nm, indicating partial shielding of the W residues due to tendency of this peptide to aggregate in aqueous solvent. These results therefore mirror the light scattering results, demonstrating self-assembly in buffer of WFF25, but not GKY25 and GKY25d. It should be noted, however, that the wavelength at maximum W fluorescence intensity for WFF25 in aqueous solution (λ_{max}=345 nm) still indicates some exposure of the W residues to the aqueous environment. Thus, the WFF25 aggregates are quite open. For GKY25 and GKY25d, λ_{max} remains unchanged in the presence of either anionic or zwitterionic liposomes (Fig. 7), demonstrating that the W

residues in these peptides are located in the polar head group region of the bilayer. For WFF25, on the other hand, there is a pronounced blue shift in the presence of anionic, but not zwitterionic, liposomes. Thus, the W residue of WFF25 is located in a more "hydrophobic" environment for the anionic liposomes. While such a result would also be compatible with the W residues being deeply buried into the acyl domain of the DOPE/DOPG membrane, the DPI results of lower membrane disordering of WFF25 than for GKY25 and GKY25d, as well previous results for W-tagged peptides (33), demonstrate a limited membrane insertion of the polarizable W residues. Given this, a more likely explanation of the W fluorescence results is the occurrence of membrane-bound WFF25 aggregates, with increased packing efficiency due to the phospholipid present, resulting in a decreased polarity in the vicinity of the W residues.

Discussion

The transition from a random coil conformation to an (amphiphilic) α-helix on peptide binding to lipid membranes has been observed in a wide range of peptides, and has also been found to be of importance to the antimicrobial activity of a number of AMPs (34). Also for GKY25, forming the C-terminal helix in human thrombin, such membrane-induced conformational transition is of some importance, evidenced by both antimicrobial effects and liposome disruption. As the helix formed is not very amphiphilic (Fig. S4) (35), however, the impaired helix formation in GKY25d has a quantitatively smaller role than for peptides undergoing more dramatic conformational changes, and/or forming helices with higher amphiphilicity, such as internal peptide segments of LL-37 (36). Nevertheless, peptide secondary structure effects in membrane interactions are shown clearly when background electrostatics is suppressed, e.g., for zwitterionic liposomes and at high ionic strength, as well in the antimicrobial effect of these peptides.

Apart from secondary structure (i.e., conformationally induced amphiphilicity), linear amphiphilicity along the peptide chain plays a major role for membrane interactions. Due to its pronounced linear amphiphilicity, WFF25 displays a considerably increased binding to anionic DOPE/DOPG bilayers compared to GKY25 and GKY25d. In contrast, WFF25 adsorption and insertion into zwitterionic DOPC and DOPC/cholesterol membranes is suppressed. A similar membrane composition selectivity was previously demonstrated for W/F-tagged peptides (37). For such end-tagged peptides, the presence of the bulky aromatic amino stretch precludes peptide insertion into zwitterionic lipid membranes as a result of a weaker electrostatic adsorption driving force, and particularly so in the presence of membrane-condensing cholesterol.

Due to its high linear amphiphilicity, WFF25 self-assembles in solution, in analogy to acyl-containing lipopeptides (38), but in contrast to highly charged and hydrophilic peptides end-functionalized with short W/F stretches (39). For the former, self-assembly has been found to limit membrane interactions and antimicrobial effects. For example, Chu-Kung et al. investigated effects of the length of fatty acids conjugated to an AKK peptide, and found the antimicrobial activity to increase with fatty acid length. They also found, however, that antimicrobial activity is lost when the minimal active concentration is higher than the critical micelle concentration (cmc) of the lipopeptide (40). In parallel, it was found that at concentrations above cmc, solution self-assembly inhibits peptide membrane binding and antimicrobial effect. Due to its intermediate mean hydrophobicity, as well as the gradual progression in polarity on going from one end of the peptide to the other, WFF25

represents a middle case between these extremes, sufficiently amphiphilic to result in self-assembly, but insufficiently so to form an essentially solvent-free micellar core. As a result of this, packing is frustrated, and can be improved by mixed aggregate formation at the membrane interface once the adsorption driving force is sufficiently high (as with the anionic DOPE/DOPG) to override the free energy penalty of placing the polarizable W/F residues in a less polar environment.

In analogy to the high binding at anionic membranes, WFF25 binds extensively to anionic non-lipid components in bacteria, notably LPS and LTA. Since LPS and LTA are both abundant components in Gram-negative and Gram-positive bacteria, respectively, they can scavenge this peptide, preventing its concentration at the membrane to reach sufficient levels to achieve efficient membrane lysis. In fact, previous studies have shown LPS to bind antimicrobial peptides with a higher affinity than lipid membranes, although with a smaller magnitude than presently observed for the highly amphiphilic WFF25 (19,41,42). In addition to such direct scavenging, preferential peptide binding to LPS and LTA may also result in an effectively impermeable layer through osmotic deswelling, in analogy to effects previously demonstrated for polyelectrolyte systems in the presence of oppositely charged peptides (43-46). Indeed, the dramatically reduced antimicrobial effect observed for WFF25 at high ionic strength, where peptide particles were considerably larger, indicates the importance also of the latter effect. Together, these effects result in an unusual discrepancy between antibacterial effects (through membrane lysis) and peptide-induced liposome leakage. Thus, for highly amphiphilic peptides such as WFF25, liposomes (also those formed by bacteria lipid extracts) do not represent a good model for bacteria.

Conclusions

Effects of peptide linear amphiphilicity on membrane interactions and antimicrobial effects were investigated for GKY25, WFF25 (with retained composition but increased linear amphiphilicity). and GKY25d (with retained sequence but suppressed conformationally induced (helix-related) amphiphilicity). These peptides incorporate into lipid membranes without insertion threshold, resulting in membrane destabilization. Similarly to AMPs end-tagged with W/F stretches, but contrary to acyl-based lipopeptides, the linear amphiphilicity of WFF25 introduces considerable selectivity between membranes of different composition. The higher binding driving force to the anionic DOPE/DOPG membrane promotes mixed aggregate formation for WFF25, not seen in the zwitterionic systems, nor for the less amphiphilic GKY25 and GKY25d. In addition, WFF25 displays extensive binding to non-lipid anionic polyelectrolytes in bacteria membranes (LPS and LTA), which thus effectively scavenge the membrane from peptide and result in decreased antimicrobial effects. Together with electrolyte-induced peptide particle growth for WFF25 and precluded passage through outer LPS and LTA layers of Gram-negative and Gram-positive bacteria, respectively, this causes an unusual lack of correlation between bacterial killing and liposome rupture for WFF25. For such highly amphiphilic peptides, liposomes (also those formed by bacteria lipid extracts) do not represent a good model for bacteria. Instead, such peptides require either work with bacteria only, or with liposomes supplemented with LPS and LTA, respectively.

Acknowledgement

This work was supported by grants from the Swedish Research Council (projects 2012-1842 and 2012-1883) and XImmune AB. Generous access to the DPI instrumentation from Biolin Farfield is greatfully acknowledged, as is valuable scientific discussion on the DPI results with Marcus Swann and Usha Devi at Biolin Farfield. Lise-Britt Wahlberg and Ann-Charlotte Strömdahl are gratefully acknowledged for skillful experimental support.

Supporting material

Peptide induced leakage for DOPE/DOPG and *E. coli* liposomes, mean liposome size in presence of peptide, CD spectra for peptides in the presence of DOPE/DOPG liposomes, a helical wheel projection of GKY25 and antimicrobial activity against *P. aeruginosa* are available as supporting material.

References

1. G.L. French, *Adv. Drug Deliv. Rev.*, 2005, **57**, 1514.
2. P.A. Lambert, *Adv. Drug Deliv. Rev.*, 2005, **57**, 1471.
3. M. Pasupuleti, A. Schmidtchen, M. Malmsten, *Crit. Rev. Biotechnol.*, 2012, **32**, 143.
4. C.J. Arnusch, R.J. Pieters, E. Breukink, *PLoS One*, 2012, **7**, e39768.
5. S. Morizane, R.L. Gallo, *J. Dermatol.*, 2012, **39**, 225.
6. J.L. Fox, *Nat. Biotechnol.*, 2013, **31**, 379.
7. R.E. Hancock, H.G. Sahl, *Nat. Biotechnol.*, 2006, **24**, 1551.
8. L.O. Brandenburg, J. Merres, L.J. Albrecht, D. Varoga, T. Pufe, *Polymers*, 2012, **4**, 539.
9. M. Koike, T. Okamoto, S. Tsuda, R. Imai, *Biochem. Biophys. Res. Commun.*, 2002, **298**, 46.
10. P. Bulet, R. Stocklin, *Protein Pept. Lett.*, 2005, **12**, 3.
11. G. Corzo, P. Escoubas, E. Villegas, K.J. Barnham, W.L. He, R.S. Norton, T. Nakajima, *Biochem. J.*, 2001, **359**, 35.
12. K. De Smet, R. Contreras, *Biotechnol. Lett.*, 2005, **27**, 1337.
13. U.H. Dürr, U.S. Sudheendra, A. Ramamoorthy, *Biochim. Biophys. Acta*, 2006, **1758**, 1408.
14. E.A. Nordahl, V. Rydengard, P. Nyberg, D.P. Nitsche, M. Morgelin, M. Malmsten, L. Bjorck, A. Schmidtchen, *Proc. Natl. Acad. Sci.*, 2004, **101**, 16879.
15. M. Malmsten, M. Davoudi, B. Walse, A. Schmidtchen, *Growth Factors*, 2007, **25**, 60.

16. P. Papareddy, V. Rydengård, M. Pasupuleti, B. Walse, M. Mörgelin, A. Chalupka, M. Malmsten, A. Schmidtchen, *PLoS Pathogens*, 2011, **6**, e1000857, 1.

17. G. Kasetty, P. Papareddy, M. Kalle, V. Rydengård, M. Mörgelin, B. Albiger, M. Malmsten, A. Schmidtchen, *Antimicrob. Agents Chemother.*, 2011, **55**, 2880.

18. M. Kalle, P. Papareddy, G. Kasetty, D.M. Tollefsen, M. Malmsten, M. Mörgelin, A. Schmidtchen, *J. Immunol.*, 2013, **190**, 6303.

19. S. Singh, M. Kalle, P. Papareddy, A. Schmidtchen, M. Malmsten, *Biomacromolecules*, 2013, **14**, 1482.

20. C. Louis-Jeune, M.A. Andrade-Navarro, C. Perez-Iratxeta, *Proteins*, 2012, **80**, 2818.

21. R.M.A. Azzam and N. M. Bashara, Ellipsometry and polarized Light, North Holland Publishing Company, Amsterdam, 1989.

22. M. Malmsten, *J. Colloid Interface Sci.*, 1994, **166**, 333.

23. M. Malmsten, N. Burns, A. Veide, *J. Colloid Interface Sci.*, 1998, **204**, 104.

24. L. Ringstad, A. Schmidtchen, M. Malmsten, *Langmuir*, 2006, **22**, 5042.

25. A. Mashagi, M. Swann, J. Popplewell, M. Textor, E. Reimhult, *Anal. Chem.*, 2008, **80**, 3666.

26. L. Yu, L. Guo, J.L. Ding, B. Ho, S.S. Feng, J. Popplewell, M. Swann, T. Wohland, *Biochim. Biophys. Acta*, 2009, **1788**, 333.

27. T.H. Lee, C. Heng, M.J. Swann, J.D. Gehman, F. Separovic, M.I. Aguilar, *Biochim. Biophys. Acta*, 2010, **1798**, 1977.

28. G. Orädd, A. Schmidtchen, M. Malmsten, *Biochim. Biophys. Acta*, 2011, **1808**, 244.

29. A.A. Strömstedt, M. Pasupuleti, A. Schmidtchen, M. Malmsten, *Biochim. Biophys. Acta*, 2009, **1788**, 1916.

30. C. Erridge, E. Bennett-Guerro, I.R. Poxton, *Microbes Infect.*, 2002, **4,** 837.

31. J.E. Baik, Y.H. Ryu, J.Y. Han, J. Im, K.Y. Kum, C.H. Yun, K. Lee, S.H. Han, *J. Endod.*, 2008, **34**, 975.

32. M.R. Eftink, *Methods Biochem. Anal.*, 1991, **35**, 127.

33. A. Schmidtchen, L. Ringstad, G. Kasetty, H. Mizuno, M.W. Rutland, M. Malmsten, *Biochim. Biophys. Acta*, 2011, **1808**, 1081.

34. A.A. Strömstedt, L. Ringstad, A. Schmidtchen, M. Malmsten, *Curr. Opinion Colloid Interface Sci.*, 2010, **15**, 467.

35. M. Schiffer, A.B. Edmundson, *Biophys. J.*, 1967, **7**, 121.

36. A. A. Strömstedt, M. Pasupuleti, A. Schmidtchen, M. Malmsten, *Antimicrob. Agents Chemother.*, 2009, **53**, 593.

37. M. Pasupuleti, A. Schmidtchen, A. Chalupka, L. Ringstad, M. Malmsten, *PLoS One*, 2009, **4**, e5285.

38. R. Jerala, *Expert Opin. Investig. Drugs.*, 2007, **16**, 1159.

39. A. Schmidtchen, M. Pasupuleti, M. Morgelin, M. Davoudi, J. Alenfall, A. Chalupka, M. Malmsten, *J. Biol. Chem.*, 2009, **284**, 17584.

40. A.F. Chu-Kung, R. Nguyen, K.N. Bozelli, M. Tirrell, *J. Colloid Interface Sci.*, 2010, **345**, 160.

41. S. Singh, G. Kasetty, A. Schmidtchen, M. Malmsten, *Biochim. Biophys. Acta*, 2012, **1818**, 2244.

42. S. Singh, P. Papareddy, M. Kalle, A. Schmidtchen, M. Malmsten, *Biochim. Biophys. Acta*, 2013, **1828**, 2709.

43. H. Bysell, P. Hansson, A. Schmidtchen, M. Malmsten, *J. Phys. Chem. B*, 2010, **114**, 1307.

44. H. Bysell, A. Schmidtchen, M. Malmsten, *Biomacromolecules*, 2009, **10**, 2162.

45. H. Bysell, M. Malmsten, *Langmuir*, 2006, **22**, 5476.

46. H. Bysell, P. Hansson, M. Malmsten, *J. Phys. Chem. B*, 2010, **114**, 7207.

47. J. Kyte, R.F. Doolittle, *J. Mol. Biol.*, 1982, **157**, 105.

Table 1. Primary structure and key properties of the peptides investigated.

Peptide Variants	*Sequence*	*IP*[1]	Z_{net}[2] *(pH 7.4)*	*H*[3]
GKY25	GKYGFYTHVFRLKKWIQKVIDQFGE	10.11	+3	- 0.52
GKY25d[4]	GKYG(f)YTH(v)FRL(k)KWI(q)KVI(d)QFGE	10.11	+3	- 0.52
WFF25	WFFFYYLIIGGGVVTHQQRKKKKDE	10.11	+3	- 0.52

[1]IP: isoelectric point; [2]Z_{net}: net charge; [3]H mean hydrophobicity on the Kyte-Doolittle scale (47); [4]D substitutions denoted lower case.

Table 2. K2D3 analysis results of CD spectra for the indicated peptides in 10 mM Tris, pH 7.4, in the absence and presence of DOPE/DOPG ("PEPG") liposomes (75/25 mol/mol) at 100 μM.

Secondary structure content (%)	GKY25		GKY25d		WFF25	
	Tris	PEPG	Tris	PEPG	Tris	PEPG
α-helix	7	33	5	1	2	1
β-strand	12	20	22	34	39	31

Figure Captions

Figure 1. Peptide binding, measured by ellipsometry, to supported DOPE/DOPG (75/25 mol/mol) bilayers in 10 mM Tris, pH 7.4, with additional 150 mM NaCl.

Figure 2. Peptide-induced membrane disordering, measured by DPI, for supported (A) DOPE/DOPG (75/25 mol/mol), (B) DOPC, and (C) DOPC/cholesterol (60/40 mol/mol) bilayers. Measurements were performed in 10 mM Tris, pH 7.4, and data reported as reduction in Δn_f, the lipid membrane birefringence (due to peptide insertion), as a function of the adsorption density of the peptide. (For DOPC, the peptide binding was interrupted by membrane detachment of weakly attached DOPC at sufficiently high peptide binding.)

Figure 3. Peptide-induced liposome leakage, measured by fluorescence spectroscopy, for (A) DOPE/DOPG (75/25 mol/mol), (B) DOPC, and (C) DOPC/cholesterol (60/40 mol/mol) in 10 mM Tris, pH 7.4.

Figure 4. Antimicrobial activity against *E. coli* (A) and *S. aureus* (B) as determined by viable count assay in 10 mM Tris, pH 7.4, with and without additional 150 mM NaCl.

Figure 5. Peptide adsorption, measured by ellipsometry, to LTA (A) and LPS (B) from 10 mM Tris, pH 7.4, with additional 150 mM NaCl.

Figure 6. Mean aggregate size, measured by dynamic light scattering, of peptides at concentration of 10 μM in 10 mM Tris, pH 7.4, with and without additional 150 mM NaCl.

Figure 7. Change in maximum wavelength tryptophan fluorescence ($\Delta\lambda_{max}$), measured by fluorescence spectroscopy, for 10 μM of the indicated peptides in the presence of DOPE/DOPG (75/25 mol/mol), DOPC, and DOPC/cholesterol (60/40 mol/mol) at 100 μM lipid in 10 mM Tris, pH 7.4.

Figure 1.

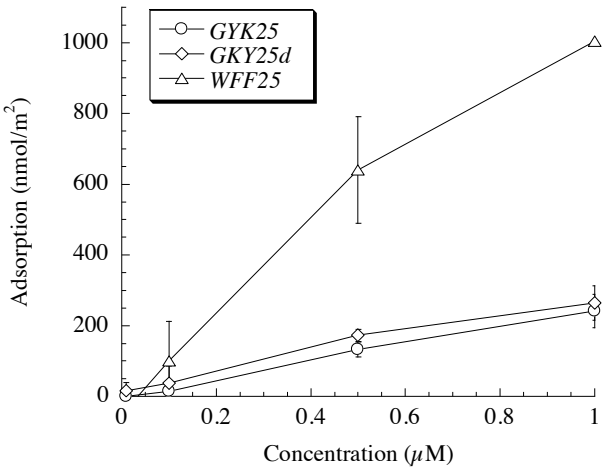
GYK25
GKY25d
WFF25
Adsorption (nmol/m2)
1000
800
600
400
200
0
0
0.2
0.4
0.6
0.8
1
Concentration (μM)

Figure 2.

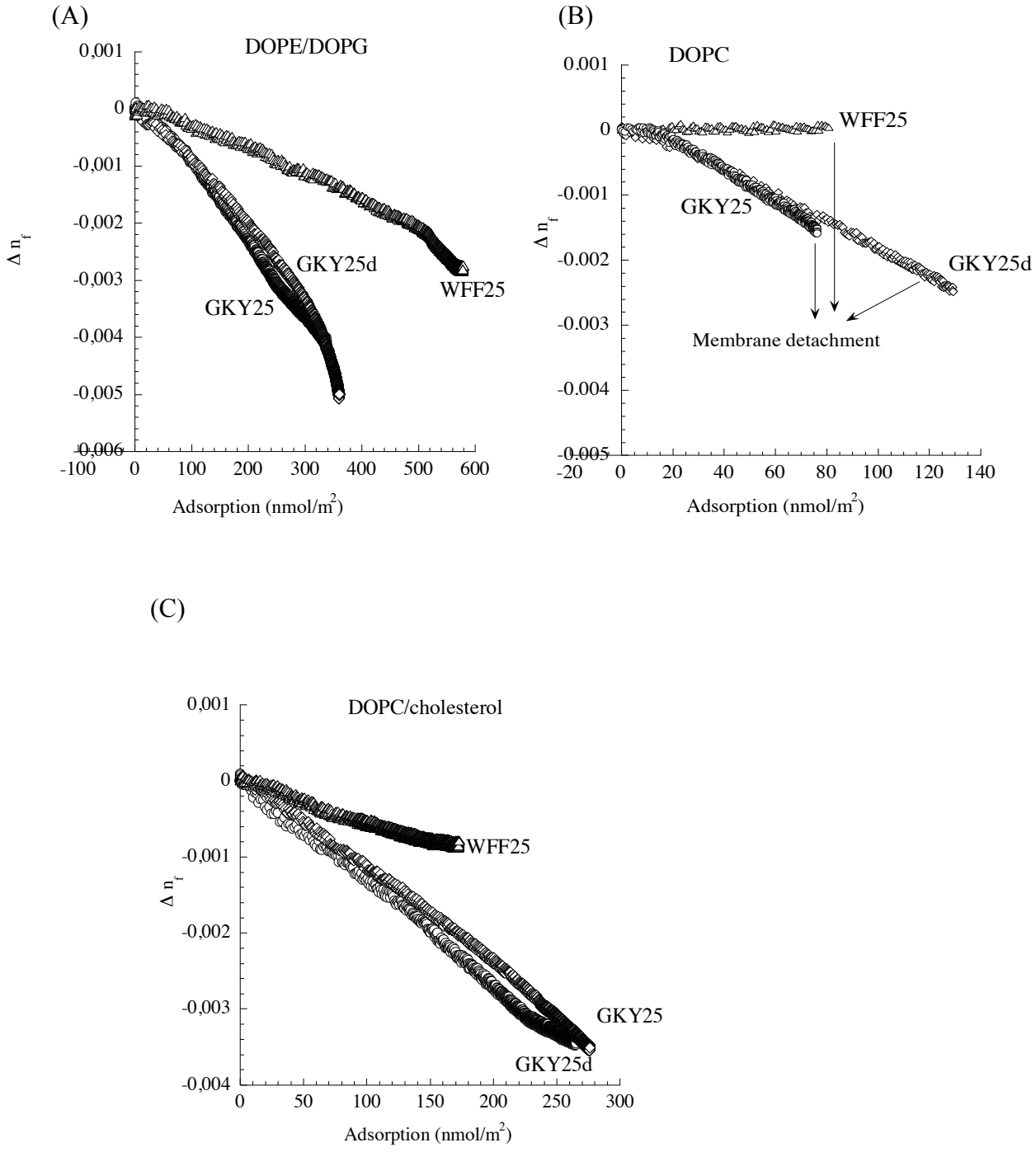
(A)
DOPE/DOPG
0,001
0
-0,001
-0,002
-0,003
-0,004
-0,005
-0,006
Δ n f
GKY25d
WFF25
GKY25
-100 0 100 200 300 400 500 600
Adsorption (nmol/m2)
(B)
DOPC
0.001
0
-0.001
-0.002
-0.003
-0.004
-0.005
Δ n f
WFF25
GKY25
GKY25d
Membrane detachment
-20 0 20 40 60 80 100 120 140
Adsorption (nmol/m2)
(C)
DOPC/cholesterol
0,001
0
-0,001
-0,002
-0,003
-0,004
Δ n f
WFF25
GKY25
GKY25d
0 50 100 150 200 250 300
Adsorption (nmol/m2)

Figure 3.

(A)

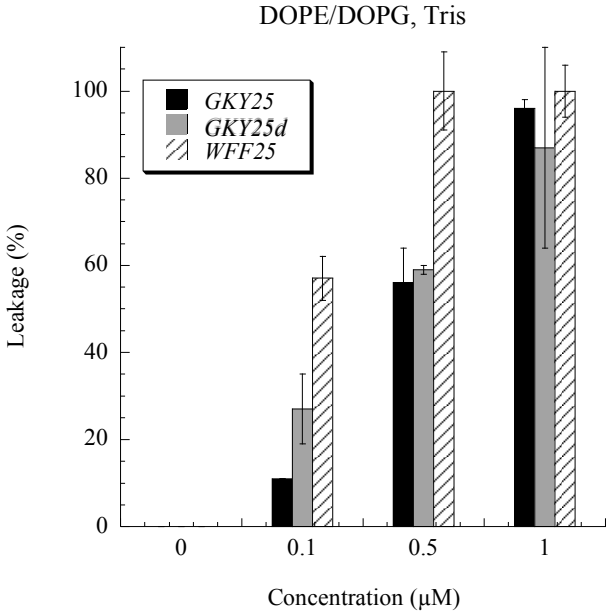
DOPE/DOPG, Tris
GKY25
GKY25d
WFF25
Leakage (%)
0
20
40
60
80
100
0
0.1
0.5
1
Concentration (μM)

(B)

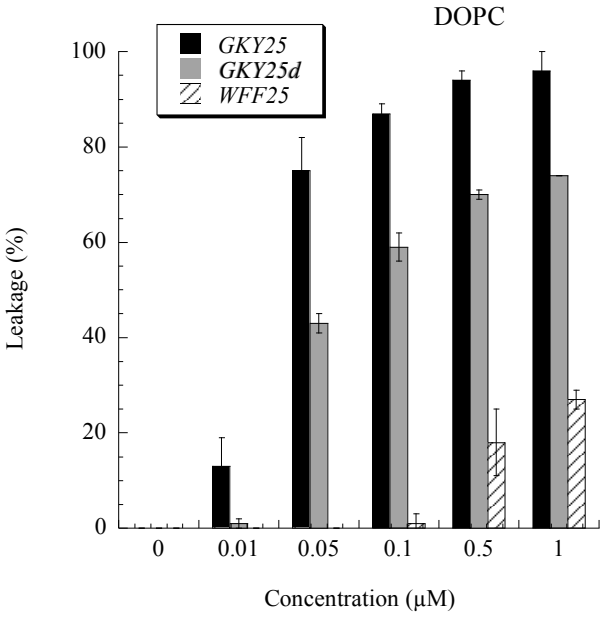
DOPC
GKY25
GKY25d
WFF25
Leakage (%)
0
20
40
60
80
100
0
0.01
0.05
0.1
0.5
1
Concentration (μM)

(C)

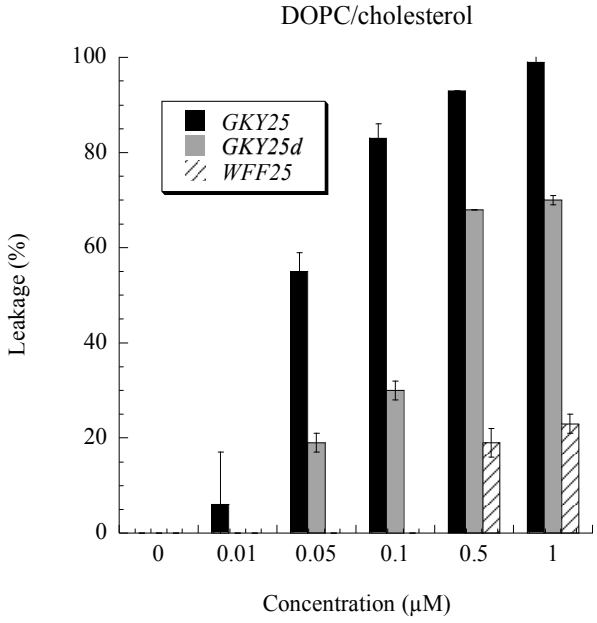
DOPC/cholesterol
GKY25
GKY25d
WFF25
Leakage (%)
0
20
40
60
80
100
0
0.01
0.05
0.1
0.5
1
Concentration (μM)

Figure 4.

(A)

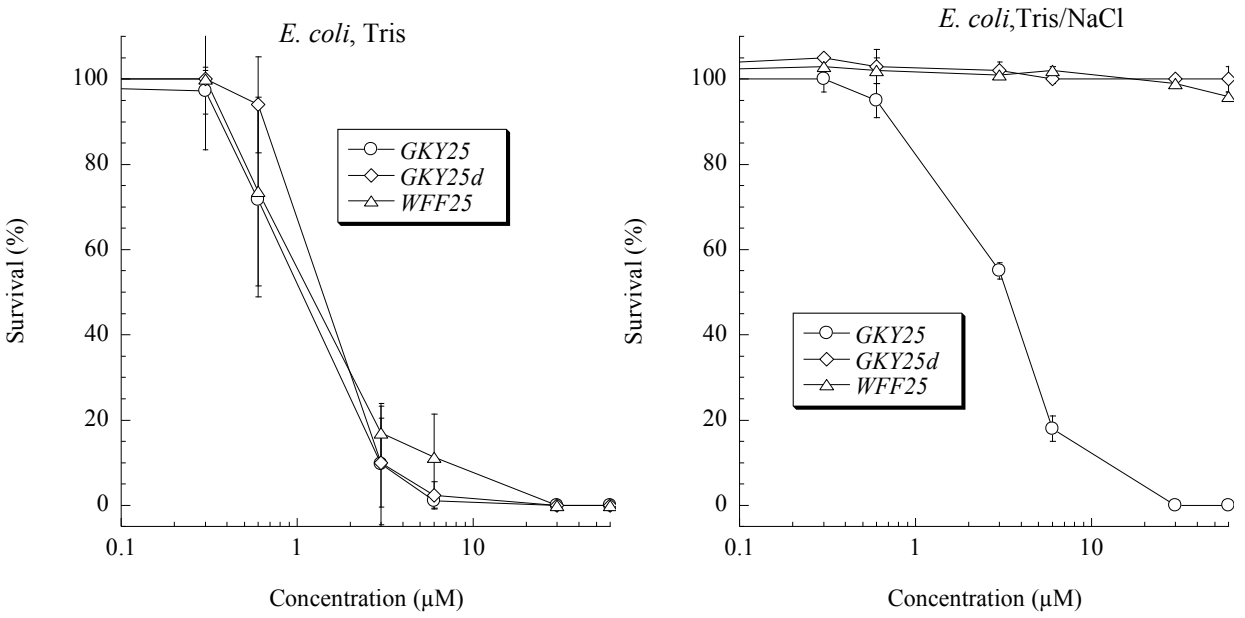
E. coli, Tris
E. coli,Tris/NaCl
GKY25
GKY25d
WFF25
Survival (%)
Concentration (μM)
0
20
40
60
80
100
0.1
1
10

(B)

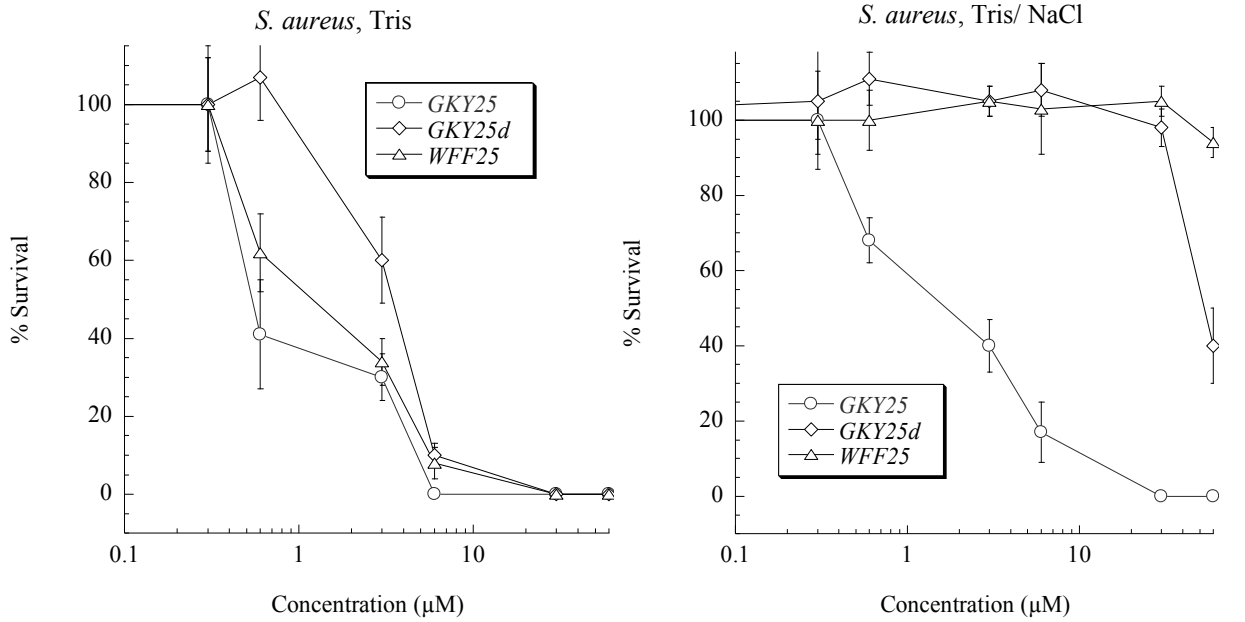
S. aureus, Tris
S. aureus, Tris/ NaCl
GKY25
GKY25d
WFF25
% Survival
Concentration (μM)
0
20
40
60
80
100
0.1
1
10

Figure 5.

(A)

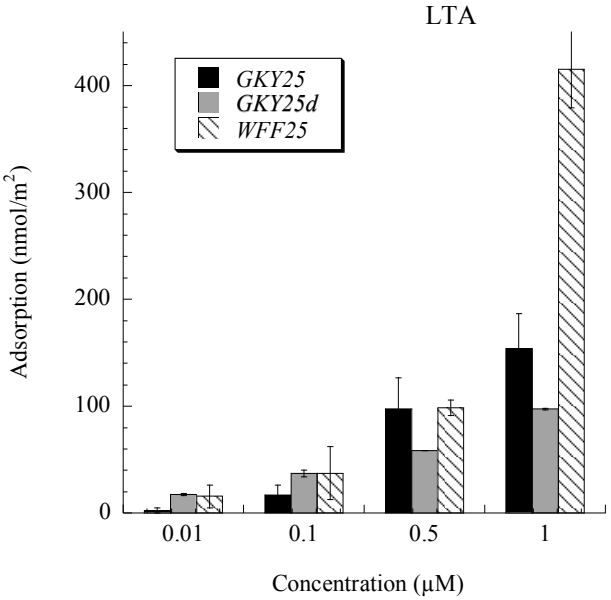
LTA
GKY25
GKY25d
WFF25
Adsorption (nmol/m2)
0
100
200
300
400
0.01
0.1
0.5
1
Concentration (μM)

(B)

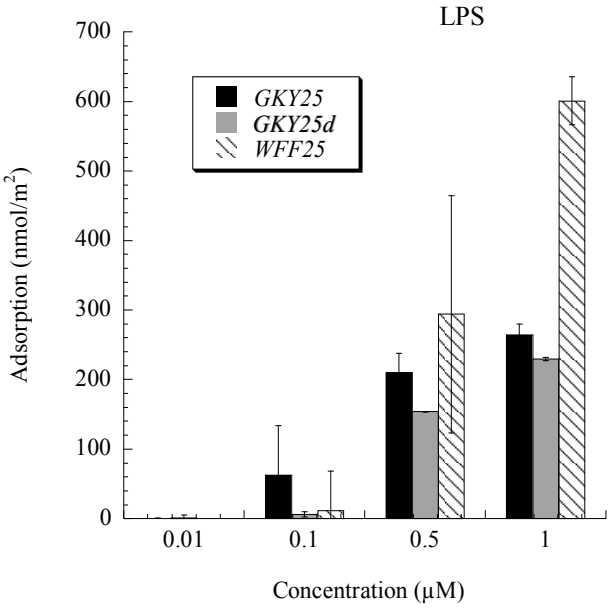
LPS
GKY25
GKY25d
WFF25
Adsorption (nmol/m2)
0
100
200
300
400
500
600
700
0.01
0.1
0.5
1
Concentration (μM)

Figure 6.

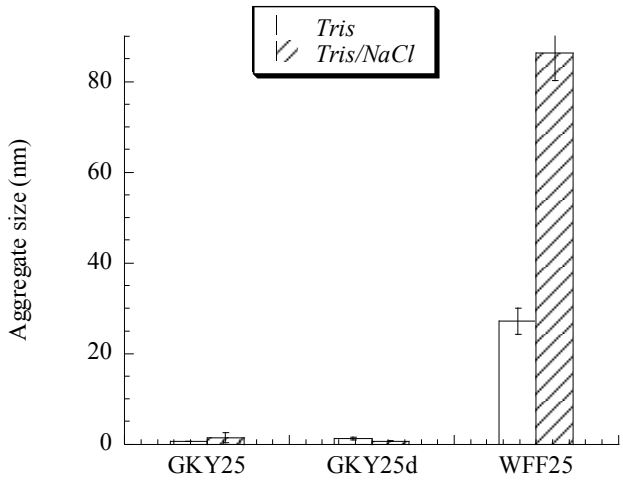
Tris
Tris/NaCl
Aggregate size (nm)
0
20
40
60
80
GKY25
GKY25d
WFF25

Figure 7.

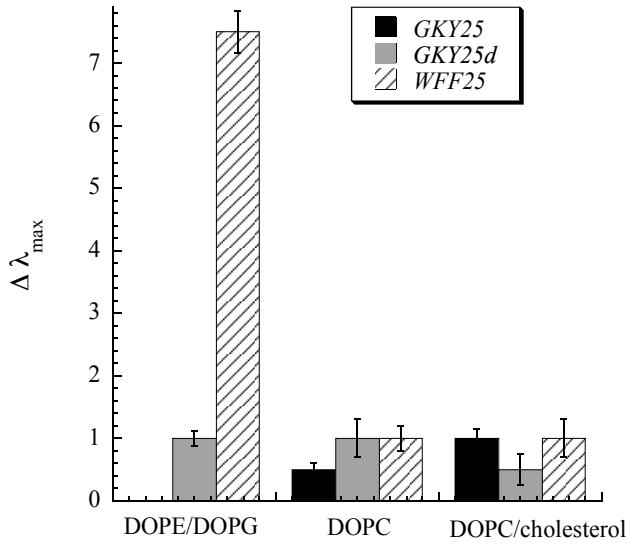
GKY25
GKY25d
WFF25
Δ λmax
0
1
2
3
4
5
6
7
DOPE/DOPG
DOPC
DOPC/cholesterol